Hindawi
International Transactions on Electrical Energy Systems
Volume 2022, Article ID 2165966, 14 pages
https://doi.org/10.1155/2022/2165966

Research Article

A Simplified Sine Cosine Algorithm for the Solution of Optimal Reactive Power Dispatch

Sushil Kumar Gupta, Manoj Kumar Kar, Lalit Kumar, and Sanjay Kumar

Department of Electrical Engineering, NIT Jamshedpur, Jamshedpur, Jharkhand, India

Correspondence should be addressed to Manoj Kumar Kar; manojkar132@gmail.com, Lalit Kumar; lalitnitjsr@gmail.com, and Sanjay Kumar; sanjay.ee@nitjsr.ac.in

Received 13 July 2022; Revised 16 October 2022; Accepted 1 November 2022; Published 15 November 2022

Academic Editor: Tianqi Hong

In this article, a simplified sine cosine algorithm (SSCA) is applied to solve the optimal reactive power dispatch (ORPD) issues by estimating the control variables. This algorithm uses sine cosine functions and generates number of random solutions to obtain the best solution by fluctuating inwards or outwards. The SSCA is implemented in the ORPD problem to find the best control variables to achieve minimum power loss and maximum net savings. Furthermore, the efficacy of SSCA is validated with other recently used algorithms considering three case studies, i.e., IEEE-30, -57, and -118 bus test system. The results show that the SSCA approach finds more precise and superior ORPD solutions. A comparison among SSCA and other methods proves the robustness of SSCA to attain the solution with faster convergence. The statistical analysis is performed to justify the effectiveness of SSCA by yielding minimum operating cost and maximum net savings as compared to other techniques considered in this study.

1. Introduction

With the increased growth of industrial and residential load demand, the transmission network has become stressed. The construction of new generating stations is not reccommended because of environmental and economic factors. Hence, the power transfer ability of the transmission lines has to be enhanced by the effective use of the existing networks. Since the last few decades, FACTS devices emerged to improve the performance of the power system by changing the AC transmission parameters [1].

The steady state network condition is determined by using power flow analysis [2]. The loading condition can be easily predicted from the power flow in the lines [3]. Nonlinear algebraic equations are used to express the steady state and reactive power supplied by a bus in a power network. As a result, iterative approaches are utilized to solve these equations [4]. FACTS devices, on the other hand, are used in the power system to improve and maintain many characteristics such as generation cost, transmission losses, system load ability, and voltage stability in both the power and distribution systems. The location, type, and rating of the devices all have an impact on how the system operates and responds. The metaheuristic algorithms draw the attention of researchers because of their efficient computational capabilities. The purpose of this article is to optimize the device's position or placement, as well as its type and size using efficient optimization algorithms.

The importance of optimal reactive power dispatch (ORPD) in modern energy management systems has piqued the interest of the research community in the power sector, with the goal of reducing real power losses and improving bus voltage while preserving load demand and operating constraints [5]. The ORPD is a nonlinear optimization problem that involves continuous and discrete control variables satisfying both equality and inequality constraints. ORPD plays a major role in economic and reliable power supply. FACTS devices mitigate the network overloading and ORPD problems when it is optimally placed [6]. The ORPD problem was solved by using PSO [7], DE [8], BBO [9], and MFO [10,11]. Some researchers used distributed generation for minimizing loss [12,13]. The solution of

optimal power flow (OPF) problem and voltage profile enhancement has been achieved incorporating some renewable sources [14–16]. However, the renewable generations are not predictable. Hence, the use of existing system to fulfill the load demand becomes the main challenge for power engineers. To examine the impact of static VAR compensator (SVC) and thyristor-controlled series capacitor (TCSC), the ORPD issue with a UPFC model was addressed utilizing lightning attachment procedure optimization [17,18]. The optimal solution was obtained in [19] with less computation time using the sine cosine algorithm. The OPF problem has been solved using an improved MFO algorithm in [20]. This algorithm was applied to different standard test bus systems with various single and multiobjective functions considered as case studies. In [21], the efficacy of MFO algorithm is justified considering various active and reactive load conditions for an IEEE-30 bus system. A fuzzy-based PSO is applied to solve the OPF problem considering different practical constraints [22]. The voltage profile was found to be enhanced by applying GSA in [23], considering nominal and contingency conditions. The maximum load ability was achieved by incorporating FACTS controllers with an objective to minimize cost in [24]. To achieve the same, the authors used a hybrid ALMF-SS method and tested on the standard IEEE-6 and IEEE-30 bus system. The self-adaptive DE approach is utilized to provide high-quality solutions to single-objective and multiobjective optimal power flow problems [25]. To handle the current stochastic OPF problems with renewable generators, a new form of the DE method is suggested in [26]. A PSO-TS hybrid technique [27] and diversity-enhanced PSO [28] is utilized to find the control variable settings that minimize transmission active power losses and load bus voltage variations. However, no literature discussed the ORPD problems considering both active and reactive loading. A modified DE method is utilized to find the solutions to ORPD problem considering three standard test systems [29].

1.1. Research Contributions. The contribution of the proposed work is summarized as follows:

(1) A simplified SCA (SSCA) algorithm is proposed that combines the exploration capability of SCA/rand-target updating schemes with the exploitation capability of SCA/best-target updating schemes through the parallel use of sine cosine operators

(2) The effectiveness of the proposed SSCA approach is assessed using 13 benchmark unimodal and multimodal functions

(3) As comparison techniques, SCA, BBO, MFO, and PSO, the four promising metaheuristic algorithms, are used

(4) Minimizing the active power loss and operating cost

(5) The IEEE-30, -57, and -118 test bus systems are used to assess the performance of the proposed SSCA under various active and reactive loading scenarios

The outlines of this paper are as follows: problem formulation is given in Section 2, the description of proposed SSCA is described in Section 3, the discussion of simulation results is explained in Section 4, and the research findings of this work is concluded in Section 5.

2. Problem Formulation

The prime objective of ORPD is to reduce both the active power loss (APL) and the operational cost by maintaining the operational limits. ORPD is mathematically modeled as a mixed integer nonlinear and nonconvex optimization program. The solution of ORPD has to be optimized because of the nonlinearity behavior of both the objective function and constraints.

The APL of the transmission line which has to be minimized can be expressed mathematically as

$$\underset{p_{\text{Loss}}}{\text{Minimize}} = \sum_{i,j\in N} G_{ij}\left[V_i^2 + V_j^2 - 2V_iV_j\cos\left(\delta_i - \delta_j\right)\right], \quad (1)$$

where G_{ij} represents the line conductance between the i^{th} and j^{th}bus, N is the number of buses, V_i and V_j represents the sending and receiving end voltages, respectively, and δ_i and δ_j represents the sending and receiving end voltages angle, respectively.

The cost minimization function can be written as

$$\text{Cost}_{\text{total}} = \text{Cost}_{\text{energy}} + \text{Cost}_{\text{facts}}, \quad (2)$$

where $\text{Cost}_{\text{energy}} = p_{\text{Loss}} \times \text{Energy rate}$ and $\text{Energy rate} = 0.06 \times 100000 \times 365 \times 24$.

Cost due to energy loss is 0.06\$/kWh, the capital cost of shunt capacitor is 1000\$, the number of hours per day is 24, and the number of days in a year is 365. Equation (2) signifies the operating cost.

$$\text{Cost}_{\text{facts}} = \text{Cost}_{\text{SVC}} + \text{Cost}_{\text{TCSC}},$$

$$\text{Cost}_{\text{SVC}} = 0.0003\left(\text{SVC}_{\text{value}}\right)^2 - 0.3051\left(\text{SVC}_{\text{value}}\right) + 127.38\text{US} \quad (3)$$

The following equality and inequality constraints must be satisfied in order to minimize the above objective function.

2.1. Equality Constraints. In most cases, the load flow balancing equations are expressed by equality constraints. (4) and (5) signifies the power balance equations satisfying the equality constraints as shown below:

$$P_{gi} - P_{di} - V_i\sum_{j=1}^{N} V_j\left[G_{ij}\cos\left(\delta_i - \delta_j\right) + B_{ij}\sin\left(\delta_i - \delta_j\right)\right] = 0, \quad (4)$$

$$Q_{gi} - Q_{di} - V_i\sum_{j=1}^{N} V_j\left[G_{ij}\sin\left(\delta_i - \delta_j\right) - B_{ij}\cos\left(\delta_i - \delta_j\right)\right] = 0, \quad (5)$$

where P_{gi} and P_{di} are the active power with respect to generation and load demand of i^{th} bus, respectively; Q_{gi} and Q_{di} are the reactive power with respect to Generation and demand of i^{th} bus, respectively; and G_{ij} and B_{ij} are the

conductance and susceptance of the lines connected to i^{th} and j^{th} bus, respectively.

2.2. Inequality Constraints. The following are the power system inequality constraints that correspond to the operational control variables.

The real power generation, reactive power generation, and voltage limit for the generator at ith bus is represented by equation (5), (6), and (7), respectively, as

$$P_{gi}^{\min} \le P_{gi} \le P_{gi}^{\max}, \tag{6}$$

where i=1,2,. . .,n_{PV}, and

$$Q_{gi}^{\min} \le Q_{gi} \le Q_{gi}^{\max}, \tag{7}$$

where i=1,2,. . .,n_{PV}, and

$$V_{gi}^{\min} \le V_{gi} \le V_{gi}^{\max}, \tag{8}$$

where i=1,2,. . .,n_{PV}.

Equation (9) signifies the the tap setting of ith transformers; $T_i^{\min}$ and $T_i^{\max}$ are the minimum and maximum tap settings of the transformer; and nT is the number of transformers, which is given as

$$T_i^{\min} \le T_i \le T_i^{\max}, \tag{9}$$

where i=1,2,. . .,n_{PV}.

Equations (10) and (11) signify the limits of SVC and TCSC. $SVC_i^{\min}$ and $SVC_i^{\max}$ are the minimum and maximum limits of SVC, whereas $TCSC_i^{\min}$ and $TCSC_i^{\max}$ are the minimum and maximum limits of TCSC, which are given as

$$\mathrm{SVC}_i^{\min} \le \mathrm{SVC}_i \le \mathrm{SVC}_i^{\max}, \tag{10}$$

where i=1,2,. . .,nS, and

$$\mathrm{TCSC}_i^{\min} \le \mathrm{TCSC}_i \le \mathrm{TCSC}_i^{\max}, \tag{11}$$

where i=1,2,. . .,nTC.

T_i denotes the i^{th} transformer's tap setting. $n_{PV}nT$, nS, and nTC represents the number of generator buses, number of transformers, number of SVC, and number of TCSC, respectively. The mathematical model of FACTS devices such as SVC and TCSC is considered same as [21].

The reactive power generations of generator (QG), tap positions of transformer (Tap), susceptance value of SVC ($0.05pu \le B\mathrm{svc} \le 0.15pu$), and reactance value of TCSC ($0.01pu \le xtcsc \le 0.06pu$) are considered as control variables.

3. Methodology

Mirjalili [20] proposed a population-based algorithm utilizing sine and cosine function and named it as the sine cosine algorithm. The simplicity and ease of implementation makes this algorithm popular. However, it suffers from slow convergence rate and fails to maintain balance between exploitation and exploration resulting in premature convergence. Hence, to overcome the demerits of SCA, we have proposed a simplified version of SCA (SSCA) using fewer parameters. Two search agent updating schemes, namely SCA/best-target and SCA/rand-target, are proposed. The SCA/best-target assists in the exploitation of search space, whereas SCA/rand-target assists in the exploration of search space. Finally, the exploitation and exploration property are combined by taking their mean and thus generating a new search agent.

In original SCA, each search agent represents a candidate solution to the problem. The solutions vary far or near the best solution. The best solution after the completion of final iteration is utilized as the solution to the problem as

$$X_i^{t+1} = \begin{cases} X_i^t + r_1 \times \sin(r_2) \times \left| r_3 \times P_i^t - X_i^t \right|, & if\ r_4 < 0.5, \\ X_i^t + r_1 \times \cos(r_2) \times \left| r_3 \times P_i^t - X_i^t \right|, & if\ r_4 \ge 0.5, \end{cases} \tag{12}$$

where X_i^t, and P_i^t represents the ith position of the current solution and destination point in tth iteration, respectively, X_i^{t+1} is the ith position of the solution in t+1 iteration, and r_1, r_2, r_3 and r_4 are the parameters of the algorithm.

Figure 1 shows the flowchart of the proposed SSCA method. The operation includes three steps: initialization of parameters, iteration step, and selection of best solution. The best search agent of the final iteration is selected as the candidate solution to the problem.

In SSCA, two proposed search agent schemes are ensembled to generate a new search agent with the parallel use of sine and cosine functions. SCA/best-target moves the search agent toward the best search agent which is shown in (13) and (14) Again, SCA/rand-target moves the search agent towards a random search agent as shown in (15) and (16) The balance between exploitation and exploration is maintained by taking the mean of these four search agents and given by equation. (16). The original SCA has four parameters, whereas the SSCA has three parameters, which helps in improving the robustness of SSCA method. The three parameters r_1, r_2, and r_3 used in SSCA are determined using equations (17), (18), and (19), respectively. The equations are shown as follows:

$$Y_1 = X_{\mathrm{best}}^t + r_1 \times \sin(r_2) \times \left| r_3 \times X_{\mathrm{rand}}^t - X_i^t \right|, \tag{13}$$

$$Y_2 = X_{\mathrm{best}}^t + r_1 \times \cos(r_2) \times \left| r_3 \times X_{\mathrm{rand}}^t - X_i^t \right|, \tag{14}$$

$$Y_3 = X_{\mathrm{rand}}^t + r_1 \times \sin(r_2) \times \left| r_3 \times X_{\mathrm{best}}^t - X_i^t \right|, \tag{15}$$

$$Y_4 = X_{\mathrm{rand}}^t + r_1 \times \cos(r_2) \times \left| r_3 \times X_{\mathrm{best}}^t - X_i^t \right|, \tag{16}$$

$$X_i^{t+1} = \mathrm{Mean}(Y_1, Y_2, Y_3, Y_4), \tag{17}$$

$$r_1 = 2 \times \left(1 - \frac{t}{T_{\max}} \right), \tag{18}$$

$$r_2 = 2 \times \mathrm{pi} \times \mathrm{rand}(0, 1), \tag{19}$$

$$r_3 = 2 \times \mathrm{rand}(0, 1), \tag{20}$$

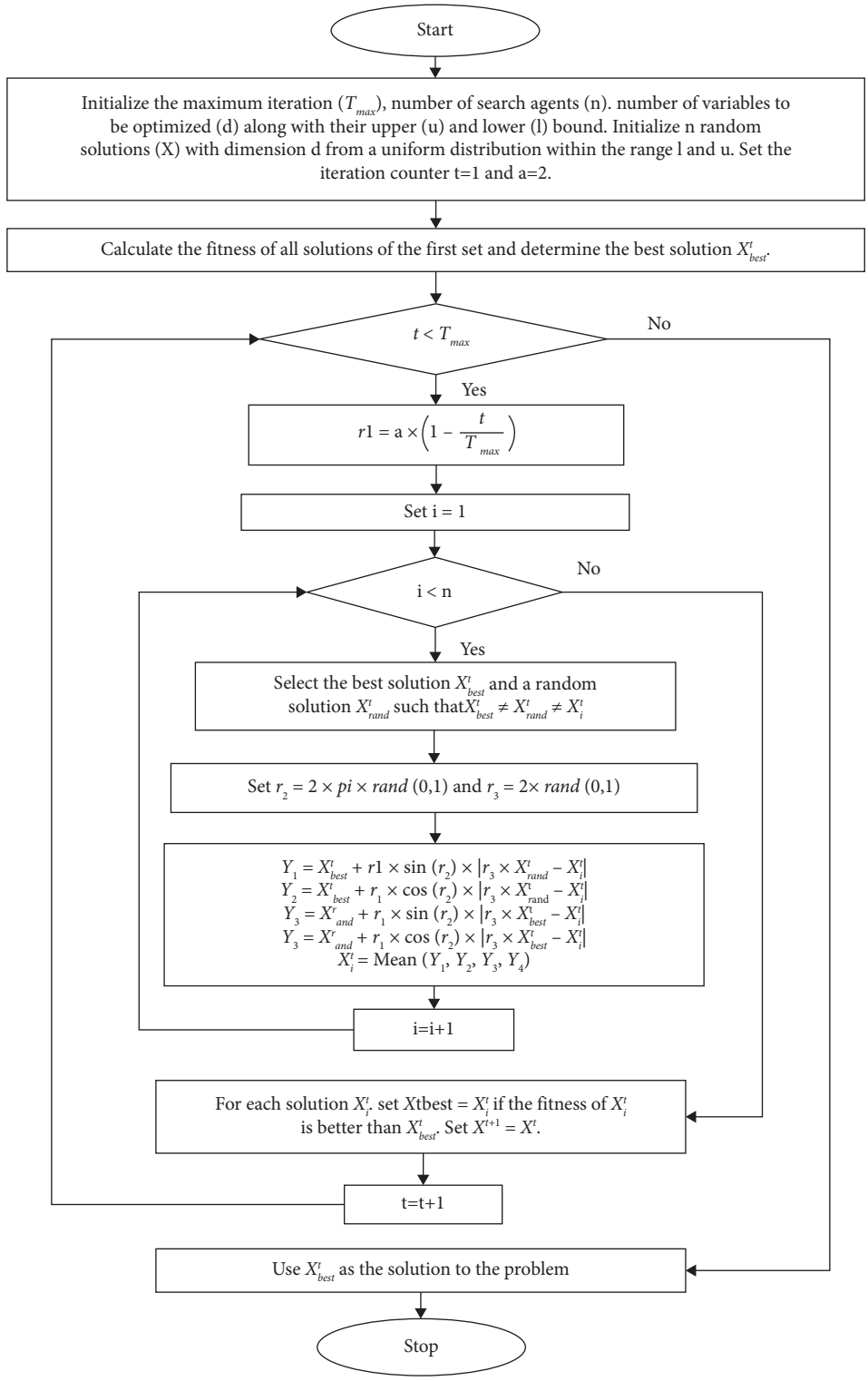

Figure 1: Flowchart for the SSCA method.

where t and $T_{\max}$ denote current iteration and maximum iteration respectively, and rand$(0, 1)$ represents the generation of a random number between 0 and 1.

The mean and standard deviation of the fitness value for different methods considering 500 iterations is evaluated and shown in Table 1. The bold face represents the best fitness value among all the methods. The proposed SSCA method is tested on various unimodal (F1–F7) and multimodal (F8–F13) functions as shown in Table 2 to justify its robustness. The proposed method gives better result in terms

Table 1: Statistical analysis of different methods (best values are presented in bold).

	SSCA Mean ± SD	SCA Mean ± SD	BBO Mean ± SD	MFO Mean ± SD	PSO Mean ± SD
F1	9.77E-29 ± 1.64E-28	1.058E-10 ± 2.048E-10	9.318E-20 ± 2.266E-19	6.217E-12 ± 1.058E-11	1.063E-18 ± 2.243E-18
F2	1.65E-17 ± 1.73E-17	3.93E-09 ± 6.24E-09	5.6E-12 ± 8.95E-12	1.78E-08 ± 2.59E-08	9.1E-13 ± 1.84E-12
F3	9.87E-17 ± 2.02E-16	0.02295 ± 0.041731	0.04077 ± 0.04197	0.657616 ± 0.441665	0.001023 ± 0.001323
F4	5.56E-10 ± 9.22E-10	0.007677 ± 0.019162	0.961993 ± 2.017756	5.546965 ± 5.085424	0.002221 ± 0.001851
F5	4.809174 ± 0.637807	7.542727 ± 0.442341	6.309724 ± 1.613368	119.3389 ± 231.1894	6.072164 ± 2.416001
F6	0.184376 ± 0.160825	0.516629 ± 0.202489	3.884666 ± 2.861071	3.89E-11 ± 1.1E-10	1.92E-20 ± 3.32E-20
F7	0.00149 ± 0.000851	0.005295 ± 0.006349	0.005182 ± 0.001862	0.019673 ± 0.014721	0.002788 ± 0.001546
F8	-2798.49 ± 172.9513	-2104.07 ± 155.2715	-3915.95 ± 189.4259	-3238.98 ± 310.8421	-2298.53 ± 346.1811
F9	0.519919 ± 1.644128	0.554686 ± 1.748545	7.987651 ± 3.170098	22.884 ± 10.14656	13.43193 ± 5.185881
F10	3E-14 ± 8E-15	0.000324 ± 0.000583	7.04E-11 ± 4.4E-11	3.51E-07 ± 1.99E-07	7.48E-11 ± 1.89E-10
F11	0.042491 ± 0.043416	0.218004 ± 0.272418	0.054998 ± 0.047894	0.139545 ± 0.087655	0.083155 ± 0.072638
F12	0.031975 ± 0.026942	0.133127 ± 0.091179	1.68E-13 ± 5.33E-13	0.311232 ± 0.587118	2.14E-20 ± 6.59E-20
F13	0.131962 ± 0.08203	0.373384 ± 0.094815	1.097407 ± 0.314339	3.731186 ± 4.656249	5.692137 ± 4.747002

Table 2: Statistical analysis of APL for IEEE 30 bus system.

Loading (P_d, Q_d)in %	Methods				
	SSCA Mean ± SD	SCA Mean ± SD	BBO Mean ± SD	MFO Mean ± SD	PSO Mean ± SD
100	0.0687 ± 0.00014	0.0697 ± 0.00037	0.0694 ± 0.00046	0.0689 ± 0.00021	0.0696 ± 0.00031
115	0.1049 ± 0.00828	0.1090 ± 0.00033	0.1086 ± 0.00034	0.1084 ± 0.0007	0.1094 ± 0.00041
125	0.1059 ± 0.01657	0.1285 ± 0.02196	0.1409 ± 0.00032	0.1407 ± 0.00002	0.1420 ± 0.00055

Table 3: WSRT results on IEEE 30 bus system.

Loading\Method	SCA	BBO	MFO	PSO
100	–	–	–	–
115	≈	≈	≈	≈
125	–	–	–	–

Table 4: Cost analysis without and with FACTS controllers for IEEE 30 bus system (best values are presented in bold).

Loading (P_d, Q_d) in %	Without FACTS controllers		With FACTS controllers		Net savings in $ (X–Y)
	APL (p. u.)	Operating cost in $ (X)	Techniques	Operating cost in $ (Y)	
100	0.0719	3779064	SSCA	3610872	168192
			SCA	3665534	113530
			BBO	3647664	131400
			MFO	3620858	158206
			PSO	3663432	115632
115	0.1120	5886720	SSCA	5513018	373702
			SCA	5729565	157155
			BBO	5708542	178178
			MFO	5698030	188690
			PSO	5749013	137707
125	0.1476	7757856	SSCA	5564527	2193329
			SCA	6751858	1005998
			BBO	7405178	352678
			MFO	7396769	361087
			PSO	7461418	296438

Table 5: Statistical analysis of APL for IEEE 57 bus system.

Loading (P_d, Q_d) in %	Methods				
	SSCA Mean ± SD	SCA Mean ± SD	BBO Mean ± SD	MFO Mean ± SD	PSO Mean ± SD
100	0.1764 ± 0.04997	0.1848 ± 0.04998	0.2503 ± 0.00316	0.2500 ± 0.00392	0.2560 ± 0.02012
115	0.3684 ± 0.10513	0.3802 ± 0.08759	0.4596 ± 0.04277	0.4256 ± 0.07231	0.4741 ± 0.05716
125	0.5241 ± 0.12698	0.6422 ± 0.09791	0.5823 ± 0.11985	0.6667 ± 0.02502	0.6013 ± 0.14315

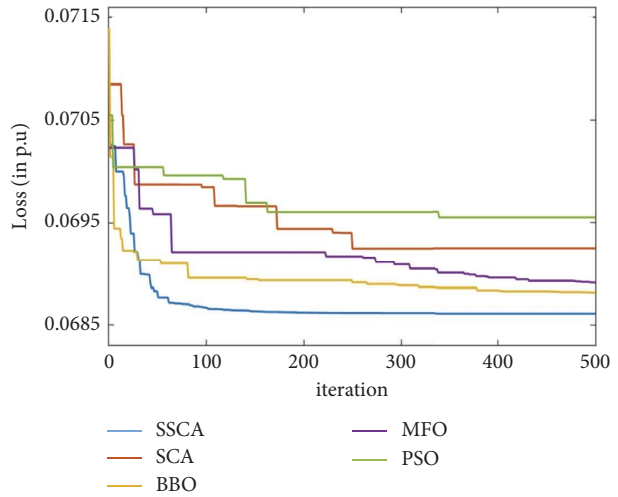

Figure 2: Loss variation in the IEEE-30 bus system at 100% loading.

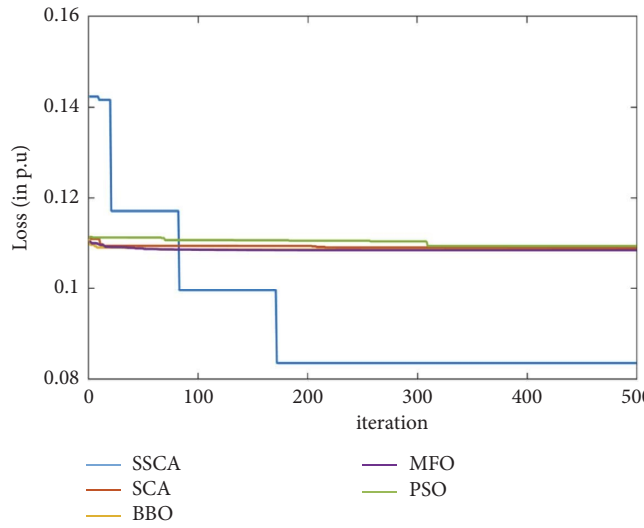

Figure 3: Loss variation in the IEEE-30 bus system at 115% loading.

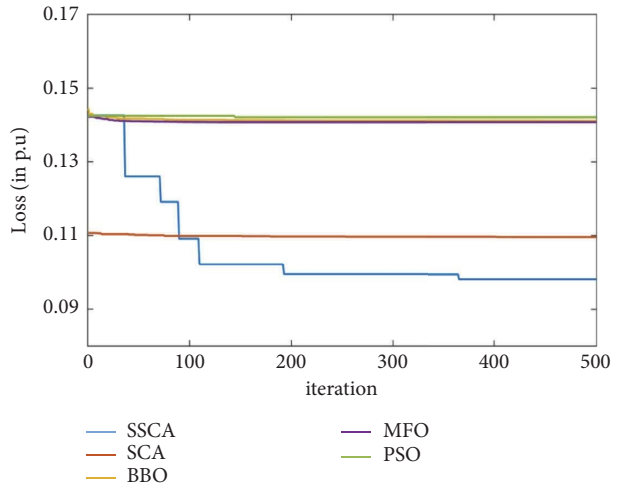

Figure 4: Loss variation in the IEEE 30 bus system at 125% loading.

Table 6: WSRT results on IEEE 57 bus system.

Loading\Method	SCA	BBO	MFO	PSO
100	≈	–	–	–
115	≈	–	≈	–
125	–	≈	–	≈

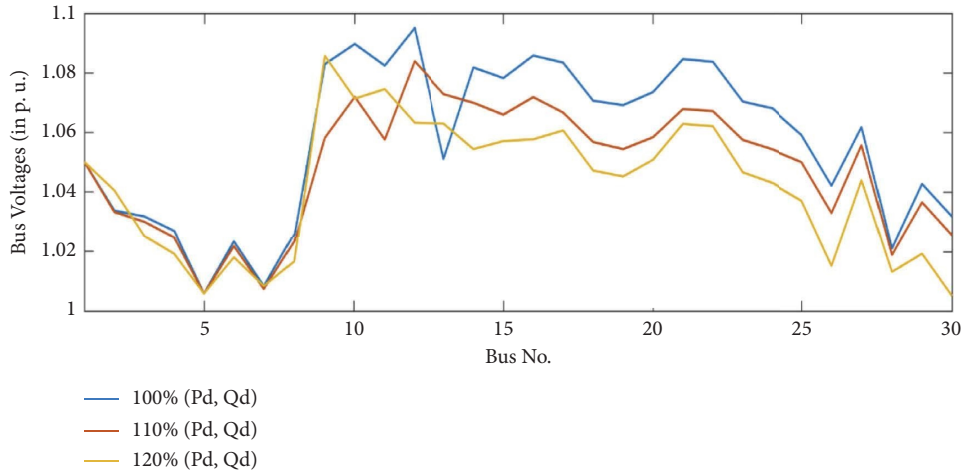

Figure 5: Bus voltage variation at different loadings in the IEEE-30 bus system.

Table 7: Cost analysis without and with FACTS controllers for IEEE 57 bus system (best values are presented in bold).

Loading (P_d, Q_d) in %	Without FACTS controllers		With FACTS controllers		Net savings in $ (X–Y)
	APL (p. u.)	Operating cost in $ (X)	Techniques	Operating cost in $ (Y)	
100	0.2955	15531480	SSCA	9271584	6259896
			SCA	9712037	5819443
			BBO	13155768	2375712
			MFO	13141051	2390429
			PSO	13453258	2078222
115	0.6876	36140256	**SSCA**	**19365206**	**16775050**
			SCA	19982260	16157996
			BBO	24158153	11982103
			MFO	22371113	13769143
			PSO	24916594	11223662
125	1.0879	57180024	SSCA	27545119	29634905
			SCA	33754032	23425992
			BBO	30606213	26573811
			MFO	35043328	22136696
			PSO	31602751	25577273

of fitness value for 10 functions (F1, F2, F3, F4, F5, F7, F9, F10, F11, and F13), whereas PSO performs better for F6 and F12 and BBO performs better for F8.

4. Results and Discussions

The performance of proposed SSCA method is demonstrated and validated considering standard IEEE-30, -57, and -118 bus test systems with different (i.e.,100%, 115%, and 125%) active and reactive loading conditions. The study is performed by using MATLAB 2019a software environment.

4.1. IEEE-30 Bus System. This system has six generators, forty-one numbers of transmission lines, four numbers of tap changing transformers, four numbers of SVC, and four numbers of TCSC [30]. The total demand of real and reactive powers is 283.4 MW and 126.2 MVAR, respectively, at 100 MVA. At first, three different active and reactive loadings (i.e., 100%, 115%, and 125%) are considered, and APL and the corresponding operating cost are calculated. Next, the weak buses and weak branches are detected by using power flow analysis. The weak buses are chosen for the placement of SVC and the weak branches are chosen for the placement

Table 8: Statistical analysis of APL for IEEE 118 bus system.

Loading (P_d, Q_d) in %	Methods				
	SSCA Mean ± SD	SCA Mean ± SD	BBO Mean ± SD	MFO Mean ± SD	PSO Mean ± SD
100	1.2525 ± 0.06204	1.3328 ± 0.20809	1.2982 ± 0.00113	1.2955 ± 0.00080	1.3098 ± 0.03542
115	1.7058 ± 0.16473	1.9660 ± 0.10591	1.8123 ± 0.19234	1.7810 ± 0.16484	1.8531 ± 0.16612
125	2.2427 ± 0.24184	2.6438 ± 0.17775	2.4435 ± 0.18864	2.3232 ± 0.27546	2.4518 ± 0.31980

Table 9: WSRT results on IEEE 118 bus system.

Loading\Method	SCA	BBO	MFO	PSO
100	–	–	–	–
115	–	≈	≈	–
125	–	–	≈	≈

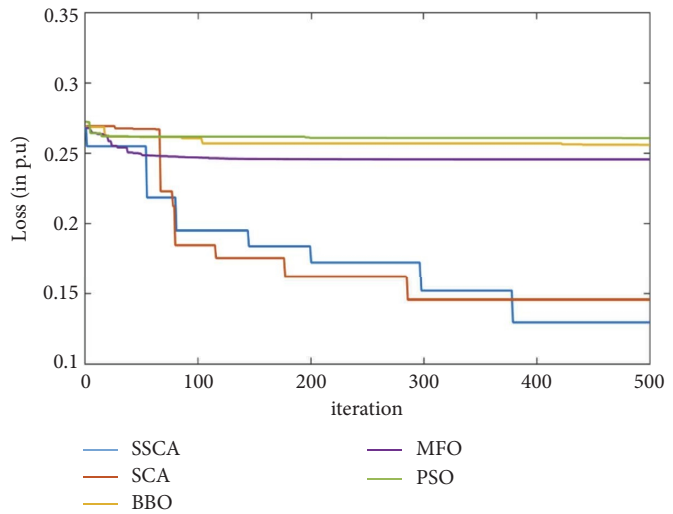

Figure 6: Loss variation in the IEEE-57 bus system at 100% loading.

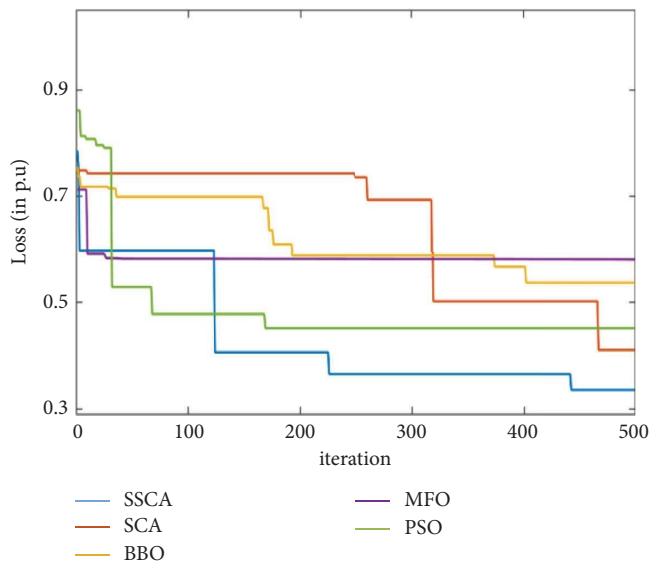

Figure 7: Loss variation in the IEEE-57 bus system at 115% loading.

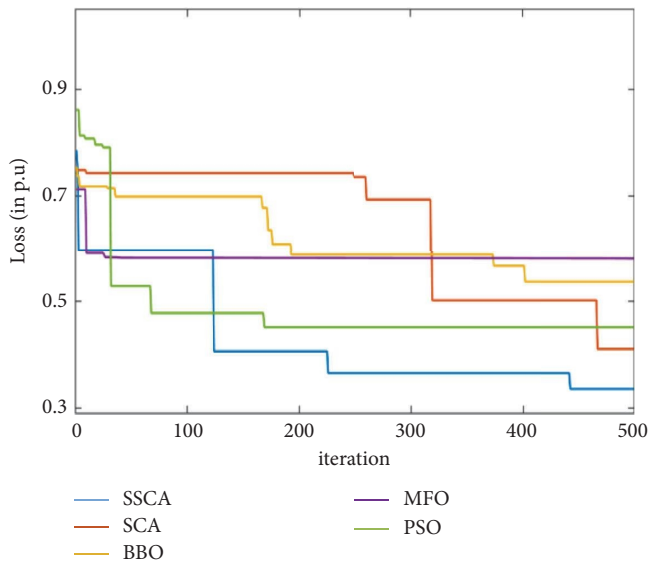

Figure 8: Loss variation in the IEEE-57 bus system at 125% loading.

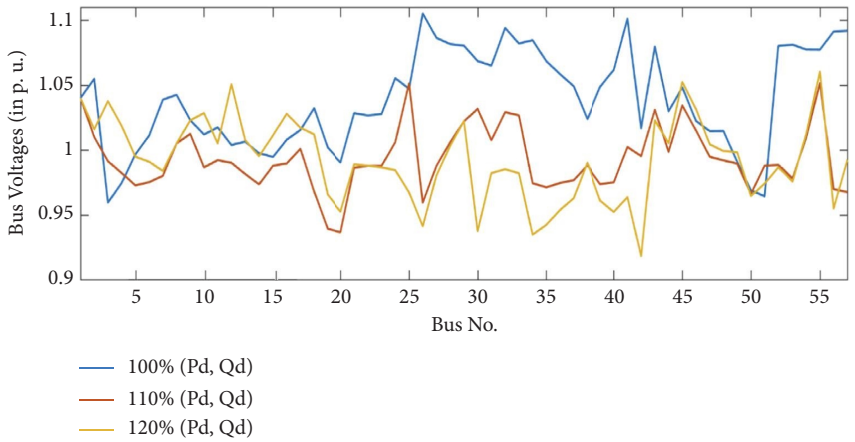

Figure 9: Bus voltage variation at different loadings in the IEEE-57 bus system.

Table 10: Cost analysis without and with FACTS controllers for IEEE 118 bus system (best values are presented in bold).

Loading (P_d, Q_d) in %)<	Without FACTS controllers		With FACTS controllers		Net savings in $ (X–Y)
	APL (p. u.)	Operating cost in $ (X)	Techniques	Operating cost in $ (Y)	
100	1.4050	73846800	SSCA	65829298	8017502
			SCA	70055121	3791679
			BBO	68234443	5612357
			MFO	68094108	5752692
			PSO	68845716	5001084
115	2.1605	113555880	SSCA	89654746	23901134
			SCA	103330332	10225548
			BBO	95253962	18301918
			MFO	93607258	19948622
			PSO	97399462	16156418
125	3.0488	160244928	SSCA	122106866	38138062
			SCA	138959179	21285749
			BBO	128428258	31816670
			MFO	131255985	28988943
			PSO	128863980	31380948

Table 11: Benchmark Functions used for performance evaluation.

Function	Formulation	Limits
Sphere [F1]	$f_1(x) = \sum_{i=1}^{N} x_i^2$	[−100, 100]
Schwefel 2.22 [F2]	$f_2(x) = \sum_{i=1}^{n} \lvert x_i \rvert + \prod_{i=1}^{n} \lvert x_i \rvert$	[−10,10]
Schwefel 1.2 [F3]	$f_3(x) = \sum_{i=1}^{n} \left(\sum_{j-1}^{i} x_j\right)^2$	[−100, 100]
Schwefel 2.21 [F4]	$f_4(x) = \max_i \{\lvert x_i \rvert,\ 1 \le i \le n\}$	[−100, 100]
Rosenbrock [F5]	$f_5(x) = \sum_{i=1}^{n-1} [100(x_{i+1} - x_i^2)^2 + (x_i - 1)^2]$	[−30, 30]
Step [F6]	$f_6(x) = \sum_{i=1}^{n} [(x_i + 0.5)]^2$	[−100, 100]
Quartic [F7]	$f_7(x) = \sum_{i=1}^{n} i x_i^4 + \text{random}(0, 1)$	[−1.28, 1.28]
Schwefel [F8]	$f_8(x) = \sum_{i=1}^{n} -x_i \sin(\sqrt{\lvert x_i \rvert})$	[−500, 500]
Rastrigin [F9]	$f_9(x) = \sum_{i=1}^{n} [x_i^2 - 10\cos(2\pi x_i) + 10]$	[−5.12, 5.12]
Ackley [F10]	$f_{10}(x) = -20\exp(-0.2\sqrt{1/n \sum_{i=1}^{n} x_i^2}) - \exp(1/n \sum_{i=1}^{n} \cos(2\pi x_i)) + 20 + e$	[−32, 32]
Griewangk [F11]	$f_{11}(x) = 1/4000 \sum_{i=1}^{n} x_i^2 - \prod_{i=1}^{n} \cos(x_i/\sqrt{i}) + 1$	[−600, 600]
Penalized [F12]	$f_{12}(x) = \pi/n\{10\sin(\pi y_1) + \sum_{i=1}^{n-1} (y_i - 1)^2 \sum[1 + 10\sin^2(\pi y_{i+1}) + (y_n - 1)^2]\} + \sum_{i=1}^{n} u(x_i, 10, 100, 4)$ where $y_i = 1 + (x_i + 1)/4$, $u(x_i, a, k, m) = \begin{cases} k(x_i - a)^m & x_i > a \\ 0 & -a < x_i < a \\ k(-x_i - a)^m & x_i < -a \end{cases}$	[−50, 50]
Penalized2 [F13]	$f_{13}(x) = 0.1\{\sin^2(3\pi x_1) + \sum_{i=1}^{n} (x_i - 1)^2[1 + \sin^2(3\pi x_i + 1)] + (x_n - 1)^2[1 + \sin^2(2\pi x_n)]\} + \sum_{i=1}^{n} u(x_i, 5, 100, 4)$	[−50, 50]

Table 12: Optimal Control Variable at various loading of IEEE 30 bus system.

Control variable\ loading	100% (P_d, Q_d)	115% (P_d, Q_d)	125% (P_d, Q_d)
Q_G (2)	0.21013	0.023858	0.45941
Q_G (5)	0.002555	0.02193	0.35855
Q_G (8)	0.30187	0.45227	0.33745
Q_G (11)	0.094829	0	0.26904
Q_G (13)	0.18351	0.40049	0.033199
Tap (11)	0.98744	0.95192	0.10439
Tap (12)	1.003	0.95308	0.99152
Tap (15)	1.013	1.0268	1.0491
Tap (36)	0.96319	0.96822	1.05
SVC (7)	0.055515	0.13158	0.1117
SVC (15)	0.084251	0.034997	0.14645
SVC (17)	0.11467	0.024353	0.14021
SVC (21)	0.10143	0.11903	0
TCSC (5)	0.06	0.052227	0.000107
TCSC (25)	0.041478	0.01413	0.011153
TCSC (28)	0.018545	0.007369	0.06
TCSC (41)	0.002778	0.017183	0.005297

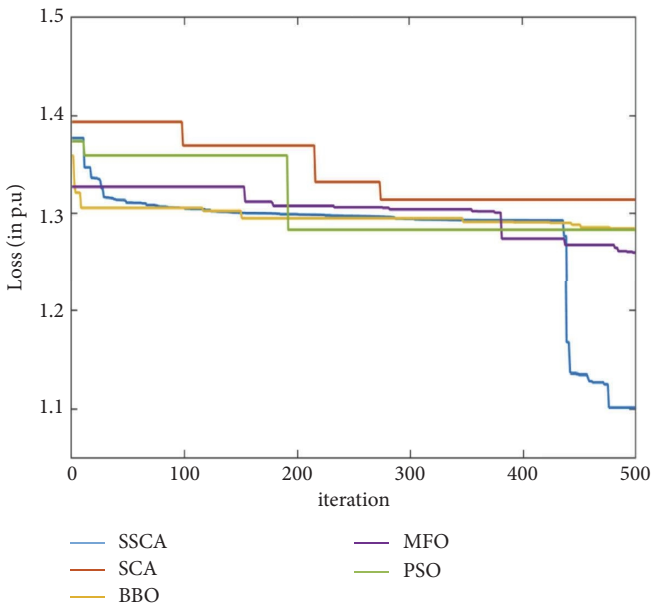

Figure 10: Loss variation in the IEEE-118 bus system at 100% loading.

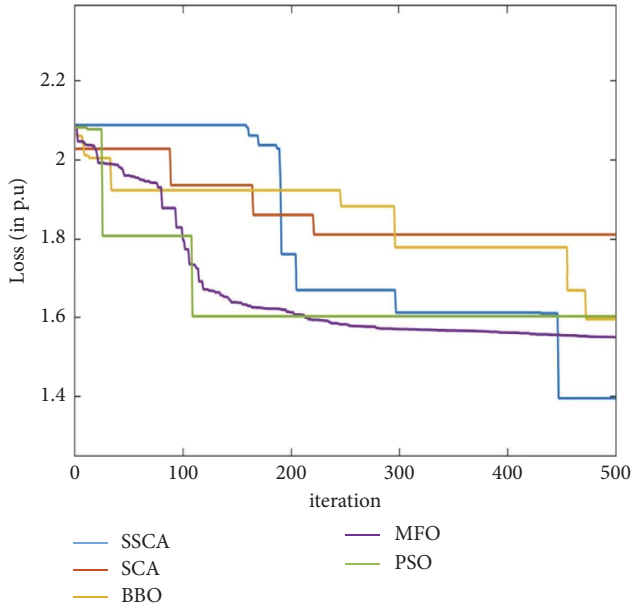

Figure 11: Loss variation in the IEEE-118 bus system at 115% loading.

of TCSC. The optimization methods are used to set the control variables. The control variables are optimized using the proposed SSCA, SCA, BBO, MFO, and PSO. Each of the aforementioned metaheuristic method is simulated 20 times, and the statistical analysis consisting mean and standard deviation values are represented in Table 3. It is noticed from Table 2 that the proposed SSCA method achieves lower loss as compared to other methods for different loading conditions. The statistical verification is justified by using WSRT analysis, as shown in Table 4. This test shows whether the proposed method is statistically inferior (−), superior (+), or equivalent (≈) when compared to other methods. A comparative analysis of APL, operating cost, and net savings without and with FACTS controllers is given in Table 5. The variations of APL at 100%, 115%, and 125% active and reactive loading cases using different metaheuristic methods are shown in Figure 2, Figures 3 and 4, respectively. The optimal control variables obtained for IEEE-30 bus system is given in Table 6. The variation of bus voltage at different loadings is shown in Figure 5. Figure 5 shows that the bus voltages are within the specified limits when FACTS devices are incorporated, thus satisfying the equality constraints.

This system has seven generators, eighty numbers of transmission lines, fifteen numbers of tap changing transformers, four numbers of SVC, and four numbers of TCSC [30]. The total demand of real and reactive powers is 1250.8 MW and 336.4 MVAR, respectively, at 100 MVA. At first, three different active and reactive loadings (i.e., 100%,

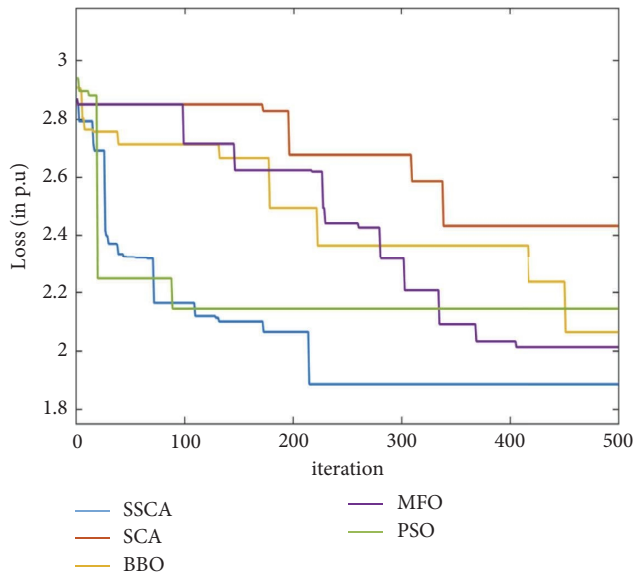

Figure 12: Loss variation in the IEEE-118 bus system at 125% loading.

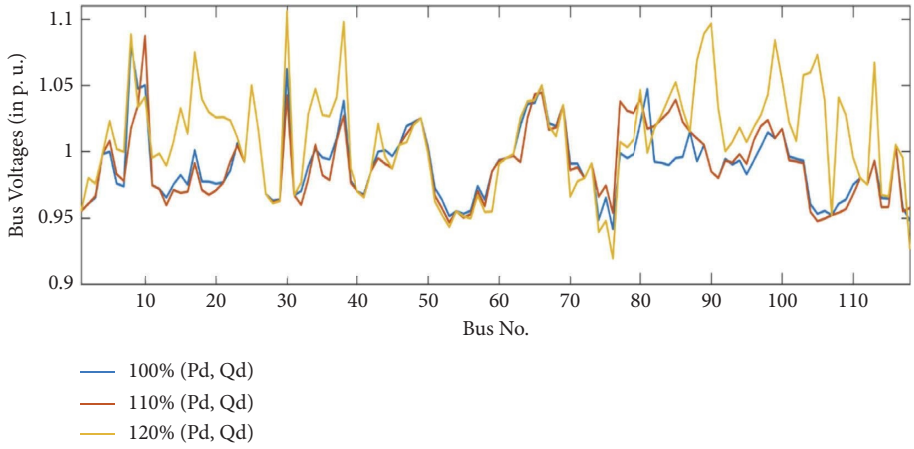

Figure 13: Bus voltage variation at different loadings in the IEEE-118 bus system.

115%, and 125%) are considered to calculate the APL and the corresponding operating cost. Next, the weak buses and weak branches are detected by using power flow analysis. The weak buses are chosen for the placement of SVC and the weak branches are chosen for the placement of TCSC. The optimization methods are used to set the control variables. The control variables are optimized using the proposed SSCA, SCA, BBO, MFO, and PSO. Each of the aforementioned metaheuristic method is simulated 20 times and the statistical analysis consisting mean and standard deviation values are represented in Table 7. It is noticed from Table 7 that the proposed SSCA method achieves lower loss as compared to other methods for different loading conditions.

The statistical verification is justified by using WSRT analysis, as shown in Table 8. This test shows whether the proposed method is statistically inferior (−), superior (+), or equivalent (≈) when compared to other methods.

A comparative analysis of APL, operating cost, and net savings without and with FACTS controllers is given in Table 9. The variations of APL at 100%, 115%, and 125% active and reactive loading cases using different metaheuristic methods are shown in Figure 6, Figures 7 and 8, respectively. The variation of bus voltage at different loadings is shown in Figure 9. Figure 9 shows that the bus voltages are within the specified limits when FACTS devices are incorporated, thus satisfying the equality constraints.

This system has fifty-three generators, one hundred eighty-six numbers of transmission lines, nine numbers of tap changing transformers, five numbers of SVC, and five numbers of TCSC [30]. The total demand of real and reactive powers is 4242 MW and 1438 MVAR, respectively, at 100 MVA. At first, three different active and reactive loadings (i.e., 100%, 115%, and 125%) are considered, and the APL and the corresponding operating cost are calculated. Next, the weak buses and weak branches are detected by using

power flow analysis. The weak buses are chosen for the placement of SVC and the weak branches are chosen for the placement of TCSC. The optimization methods are used to set the control variables. The control variables are optimized using the proposed SSCA, SCA, BBO, MFO, and PSO. Each of the aforementioned metaheuristic method is simulated 20 times, and the statistical analysis consisting mean, standard deviation, values are represented in Table 10. It is noticed from Table 10 that the proposed SSCA method achieves lower loss as compared to other methods for different loading conditions.

The statistical verification is justified by using WSRT analysis, as shown in Table 11. This test shows whether the proposed method is statistically inferior (−), superior (+), or equivalent (≈) when compared to other methods.

A comparative analysis of APL, operating cost, and net savings without and with FACTS controllers is given in Table 12. The variations of APL at 100%, 115%, and 125% active and reactive loading cases using different metaheuristic methods are shown in Figure 10, Figures 11 and 12, respectively. The variation of bus voltage at different loadings is shown in Figure 13. Figure 13 shows that the bus voltages are within the specified limits when FACTS devices are incorporated, thus satisfying the equality constraints.

5. Conclusion

In this paper, the ORPD problems are solved by using a novel SSCA method. Three test bus systems such as IEEE-30, -57, and -118 bus system is considered as case studies with 100%, 115%, and 125% active and reactive loadings. The SSCA method is used to provide the optimal setting of control variable parameters. The optimal positioning of FACTS controllers significantly reduces the net savings. The efficacy of the proposed SSCA method is validated in achieving lower real power loss and hence operating cost. From the simulation results, it is clear that the SSCA method is capable to reduce losses as compared to the other methods. The WSRT result shows the statistical supremacy of proposed SSCA over other methods. Therefore, the SSCA method may be used for solving the real-world problems. [31–33]

Data Availability

The data that support the findings of this study are available from the corresponding author upon reasonable request.

Conflicts of Interest

The authors declare that they have no conflicts of interest.

References

[1] N. G. Hingorani, "Flexible AC transmission," *IEEE spectrum*, vol. 30, no. 4, pp. 40–45, 1993.

[2] D. J. Gotham and G. T. Heydt, "Power flow control and power flow studies for systems with FACTS devices," *IEEE Transactions on Power Systems*, vol. 13, no. 1, pp. 60–65, 1998.

[3] B. Bhattacharyya and S. Kumar, "Loadability enhancement with FACTS devices using gravitational search algorithm," *International Journal of Electrical Power & Energy Systems*, vol. 78, pp. 470–479, 2016.

[4] A. M. Shaheen, R. A. El-Sehiemy, and S. M. Farrag, "A reactive power planning procedure considering iterative identification of VAR candidate buses," *Neural Computing & Applications*, vol. 31, no. 3, pp. 653–674, 2019.

[5] Y. Muhammad, R. Khan, M. A. Z. Raja, F. Ullah, N. I. Chaudhary, and Y. He, "Solution of optimal reactive power dispatch with FACTS devices: a survey," *Energy Reports*, vol. 6, pp. 2211–2229, 2020.

[6] P. Preedavichit and S. C. Srivastava, "Optimal reactive power dispatch considering FACTS devices," *Electric Power Systems Research*, vol. 46, no. 3, pp. 251–257, 1998.

[7] B. Zhao, C. X. Guo, and Y. J. Cao, "A multiagent-based particle swarm optimization approach for optimal reactive power dispatch," *IEEE Transactions on Power Systems*, vol. 20, no. 2, pp. 1070–1078, 2005.

[8] A. A. E. Ela, M. A. Abido, and S. R. Spea, "Differential evolution algorithm for optimal reactive power dispatch," *Electric Power Systems Research*, vol. 81, no. 2, pp. 458–464, 2011.

[9] P. K. Roy, S. P. Ghoshal, and S. S. Thakur, "Optimal reactive power dispatch considering flexible AC transmission system devices using biogeography-based optimization," *Electric Power Components and Systems*, vol. 39, no. 8, pp. 733–750, 2011.

[10] R. Ng Shin Mei, M. H. Sulaiman, Z. Mustaffa, and H. Daniyal, "Optimal reactive power dispatch solution by loss minimization using moth-flame optimization technique," *Applied Soft Computing*, vol. 59, pp. 210–222, 2017.

[11] M. K. Kar, L. Kumar, S. Kumar, and A. K. Singh, "Efficient operation of power system with FACTS controllers using evolutionary techniques," in *Proceedings of the 2020 7th International Conference on Signal Processing And Integrated Networks (SPIN)*, pp. 962–965, IEEE, Noida, India, 2020, February.

[12] B. Singh and B. J. Gyanish, "Impact assessment of DG in distribution systems from minimization of total real power loss viewpoint by using optimal power flow algorithms," *Energy Reports*, vol. 4, pp. 407–417, 2018.

[13] P. V. R. Varma, M. K. Kar, and A. K. Singh, "Optimal sizing and location of DG for power loss reduction and voltage improvement of distribution system using IHSA algorithm," in *Proceedings of the 2021 IEEE 2nd International Conference on Applied Electromagnetics, Signal Processing, & Communication (AESPC)*, pp. 1–5, IEEE, Bhubaneswar, India, November 2021.

[14] P. P. Biswas, P. Arora, R. Mallipeddi, P. N. Suganthan, and B. K. Panigrahi, "Optimal placement and sizing of FACTS devices for optimal power flow in a wind power integrated electrical network," *Neural Computing & Applications*, vol. 33, no. 12, pp. 6753–6774, 2021.

[15] A. Tripathy and M. K. Kar, "Voltage profile enhancement of a 33 bus system integrated with renewable energy sources and electric vehicle," in *Proceedings of the 2021 8th International Conference on Signal Processing And Integrated Networks (SPIN)*, pp. 281–286, IEEE, 2021.

[16] M. Ebeed, A. Alhejji, S. Kamel, and F. Jurado, "Solving the optimal reactive power dispatch using marine predators algorithm considering the uncertainties in load and wind-solar generation systems," *Energies*, vol. 13, no. 17, p. 4316, 2020.

[17] M. A. Taher, S. Kamel, F. Jurado, and M. Ebeed, "Optimal power flow solution incorporating a simplified UPFC model using lightning attachment procedure optimization," *International Transactions on Electrical Energy Systems*, vol. 30, no. 1, Article ID e12170, 2020.

[18] N. H. Khan, Y. Wang, D. Tian et al., "A novel modified lightning attachment procedure optimization technique for optimal allocation of the FACTS devices in power systems," *IEEE Access*, vol. 9, pp. 47976–47997, 2021.

[19] A. F. Attia, R. A. El Sehiemy, and H. M. Hasanien, "Optimal power flow solution in power systems using a novel Sine-Cosine algorithm," *International Journal of Electrical Power & Energy Systems*, vol. 99, pp. 331–343, 2018.

[20] M. A. Taher, S. Kamel, F. Jurado, and M. Ebeed, "An improved moth-flame optimization algorithm for solving optimal power flow problem," *International Transactions on Electrical Energy Systems*, vol. 29, no. 3, Article ID e2743, 2019.

[21] L. Kumar, M. K. Kar, and S. Kumar, "Reactive power management by optimal positioning of FACTS controllers using MFO algorithm," in *Proceedings of the 2021 Emerging Trends in Industry*, pp. 1–6, IEEE, Raigarh, India, 2021, May.

[22] E. Naderi, M. Pourakbari-Kasmaei, and H. Abdi, "An efficient particle swarm optimization algorithm to solve optimal power flow problem integrated with FACTS devices," *Applied Soft Computing*, vol. 80, pp. 243–262, 2019.

[23] S. Duman, U. Güvenç, Y. Sönmez, and N. Yörükeren, "Optimal power flow using gravitational search algorithm," *Energy Conversion and Management*, vol. 59, pp. 86–95, 2012.

[24] S. Dash, K. R. Subhashini, and J. Satapathy, "Efficient utilization of power system network through optimal location of FACTS devices using a proposed hybrid meta-heuristic Ant Lion-Moth Flame-Salp Swarm optimization algorithm," *International Transactions on Electrical Energy Systems*, vol. 30, no. 7, Article ID e12402, 2020.

[25] H. Pulluri, R. Naresh, and V. Sharma, "An enhanced self-adaptive differential evolution-based solution methodology for multiobjective optimal power flow," *Applied Soft Computing*, vol. 54, pp. 229–245, 2017.

[26] N. H. Awad, M. Z. Ali, R. Mallipeddi, and P. N. Suganthan, "An efficient differential evolution algorithm for stochastic OPF based active–reactive power dispatch problem considering renewable generators," *Applied Soft Computing*, vol. 76, pp. 445–458, 2019.

[27] Z. Sahli, A. Hamouda, A. Bekrar, and D. Trentesaux, "Reactive power dispatch optimization with voltage profile improvement using an efficient hybrid algorithm," *Energies*, vol. 11, no. 8, p. 2134, 2018.

[28] M. Vishnu and S. K. Tk, "An improved solution for reactive power dispatch problem using diversity-enhanced particle swarm optimization," *Energies*, vol. 13, no. 11, p. 2862, 2020.

[29] M. K. Kar, S. Kumar, A. K. Singh, and S. Panigrahi, "Reactive power management by using a modified differential evolution algorithm," *Optimal Control Applications and Methods*, 2021.

[30] L. Kumar, M. K. Kar, and S. Kumar, "Statistical analysis based reactive power optimization using improved differential evolutionary algorithm," *Expert Systems*, Article ID e13091, 2022.

[31] M. Nadeem, K. Imran, A. Khattak et al., "Optimal placement, sizing and coordination of FACTS devices in transmission network using whale optimization algorithm," *Energies*, vol. 13, no. 3, p. 753, 2020.

[32] M. K. Kar, S. Kumar, A. K. Singh, and S. Panigrahi, "A modified sine cosine algorithm with ensemble search agent updating schemes for small signal stability analysis," *International Transactions on Electrical Energy Systems*, vol. 31, no. 11, Article ID e13058, 2021.

[33] S. Mirjalili, "SCA: a sine cosine algorithm for solving optimization problems," *Knowledge-Based Systems*, vol. 96, pp. 120–133, 2016.